0026-895X/07/7101-83–91$20.00
MOLECULAR PHARMACOLOGY
Copyright © 2007 The American Society for Pharmacology and Experimental Therapeutics
Mol Pharmacol 71:83–91, 2007

Vol. 71, No. 1
25015/3161582
Printed in U.S.A.

Human RNase H1 Discriminates between Subtle Variations in the Structure of the Heteroduplex Substrate

Walt F. Lima, John B. Rose, Josh G. Nichols, Hongjiang Wu, Michael T. Migawa, Tadeusz K. Wyrzykiewicz, Andrew M. Siwkowski, and Stanley T. Crooke

Department of Molecular and Structural Biology, Isis Pharmaceuticals, Carlsbad, California

Received April 3, 2006; accepted October 4, 2006

ABSTRACT

In a previous study, we demonstrated that the sugar conformation and helical geometry of the heteroduplex substrate at the catalytic site of human RNase H1 directs the selective recognition of the substrate by the enzyme (*J Biol Chem* **279:** 36317–36326, 2004). In this study, we systematically introduced 2′-methoxyethoxy (MOE) nucleotides into the antisense oligodeoxyribonucleotide (ASO) of the heteroduplex to alter the helical geometry of the substrate. The MOE substitutions at the 3′ and 5′ poles of the ASO resulted in fewer cleavage sites and slower cleavage rates compared with the unmodified substrates. Furthermore, a greater reduction in cleavage activity was observed for MOE substitutions at the 5′ pole of the ASO. The 3′- and 5′-most cleavage sites were positioned two and four to five base pairs, respectively, from the nearest MOE residues, suggesting a conformational transmission of the MOE/RNA helical geometry into the DNA/RNA portion of the heteroduplex. Similar conformational transmission was observed for Okazaki-like substrates containing deoxyribonucleotide substitutions at the 3′ pole of the oligoribonucleotide. Finally, the heteroduplex substrates exhibited preferred cleavage sites that were cleaved 2- to 3-fold faster than other sites in the substrate, and these sites exhibited the greatest influence on the initial cleavage rates. The data presented here offer further insights into the role substrate structure plays in directing human RNase H1 activity as well as the design of effective ASOs.

RNase H hydrolyzes RNA in RNA-DNA hybrids (Stein and Hausen, 1969). RNase H enzymes function as endonucleases requiring divalent cations (e.g., Mg^{2+}, Mn^{2+}) to produce cleavage products with 5′-phosphate and 3′-hydroxyl termini (Crouch and Dirksen, 1982). RNase H activity seems to be ubiquitous in eukaryotes and bacteria (Busen, 1980; Rong and Carl, 1990; Itaya and Kondo, 1991; Itaya et al., 1991; Kanaya and Itaya, 1992; Eder et al., 1993). Two classes of RNase H enzymes have been identified in mammalian cells (Busen, 1980; Masutani et al., 1990; Eder et al., 1993; Frank et al., 1994; Wu et al., 1998). Although the biological roles for the human enzymes are not fully understood, RNase H2 seems to be involved in de novo DNA replication, and RNase H1 has been shown in mice to be important for mitochondrial DNA replication (Busen et al., 1977; Turchi et al., 1994; Ceritelli et al., 2003). In addition, human RNase H1 was shown to play a dominant role in the activities of DNA-like antisense oligonucleotides (ASO) (Wu et al., 2004).

The structure of human RNase H1 consists of an RNA-binding domain homologous with yeast RNase H1 that is separated from the catalytic domain by a 62-amino acid spacer region (Cerritelli and Crouch, 1995; Evans and Bycroft, 1999; Wu et al., 2001). The catalytic domain is highly conserved with the amino acid sequences of other RNase H1 proteins and contains the key catalytic and substrate binding residues required for activity (Katayanagi et al., 1990; Yang et al., 1990; Kanaya et al., 1991; Nakamura et al., 1991; Wu et al., 2001). In addition, the catalytic domain has been shown to contain a unique redox switch formed by adjacent cysteine residues (Lima et al., 2003a). The spacer region has been shown to be required for RNase H activity (Wu et al., 2001). Although the RNA binding domain is not required for RNase H activity, this region is responsible for the enhanced binding affinity of the human enzyme for the heteroduplex substrate as well as the strong positional preference for cleavage exhibited by the enzyme (Wu et al., 2001; Lima et al., 2003b). Finally, the positional preference for cleavage is consistent with the proposed biological role for mammalian RNase H1 (i.e., the removal of RNA primers during mitochondrial DNA synthesis) (Ceritelli et al., 2003).

First-generation phosphorothioate oligodeoxynucleotides have been shown to induce pharmacological effects in vivo

Article, publication date, and citation information can be found at http://molpharm.aspetjournals.org.
doi:10.1124/mol.106.025015.

ABBREVIATIONS: ASO, antisense oligonucleotide; MOE, 2′-methoxyethoxy; PCR, polymerase chain reaction; dsDNA, double-stranded DNA; RNA-BD, RNA binding domain.

and to reduce target RNA in humans (Yacyshyn et al., 1998). However, they display significant limitations, including limited potency and the need to be given intravenously every other day. The 2′-methoxyethoxy (MOE) modified chimeric ASOs are the product of more than a decade of medicinal chemistry research of antisense oligonucleotides (for review see Crooke, 2001). MOE modifications enhance affinity for target approximately 1° to 2° per modification, improve potency by 10- to 40-fold, and extend elimination half-lives in all species, including humans, from 14 to 30 days (for review, see Crooke, 2001). MOE-modified chimeric ASOs have also been shown to interact differently with the Toll-like receptors than do the DNA ASOs; as a result, they are less pro-inflammatory (for review, see Crooke, 2001). Second-generation MOE chimeric ASOs currently in clinical trails are showing improved efficacy and therapeutic indexes in humans compared with first-generation ASOs. For example, Isis 301012 (Kastelein et al., 2006), an inhibitor of apoB100, was shown to reduce apoB100 protein, low-density lipoprotein, very-low-density lipoprotein, total cholesterol, and triglycerides in a dose-dependent fashion, with a minimum effective dose of 50 mg/week administered s.c. Consistent with an elimination half-life of 31 days, it produced effects that lasted as long as 3 months. Moreover, it was extremely well tolerated (Kastelein et al., 2006). In addition, positive phase 2 results with patients with type 2 diabetes have been reported for the protein tyrosine phosphatase 1B inhibitor Isis 113715 (Kjems et al., 2005). As another example, OGX-011 (Chi et al., 2004) produced dose-dependent reduction to greater than 90% of its target, clusterin, in prostate cancer and lymph nodes in patients with locally invasive prostate cancer (Chi et al., 2004).

The purpose of the present study was to extend our earlier observations and to provide a more precise understanding of the effects of MOE nucleotides on both the overall rate of cleavage and the precise positions of cleavage induced by human RNase H1. In a previous study, we evaluated the effects of modified nucleotides positioned at sites on the substrate that interact directly with the enzyme (Lima et al., 2004). Here, we designed a series of chimeric ASOs to evaluate the local and long-range influence of the substrate structure on human RNase H1 activity. The MOE nucleotides were selected for this study because they have been shown to enhance the potency of ASOs through increased hybridization affinity and nuclease resistance (for review, see Crooke, 2001).

Materials and Methods

Preparation of Human RNase H1. Human RNase H1 containing an N-terminal His-tag was expressed and purified as described previously (Lima et al., 2001). In brief, the plasmids were transfected into *E. coli* BL21 (DE3) (Novagen, Madison, WI). The bacteria was grown in Terrific Broth medium (Qbiogene Inc., Carlsbad, CA) at 37°C and harvested at an OD_{600} of 1.2. The cells were induced with 1 mM isopropylthiogalactoside at 37°C for 2 h. The cells were lysed in 6 M guanidine hydrochloride, 100 mM sodium phosphate, 10 mM Tris, pH 8.0 for 16–20 h at 24°C. The recombinant proteins were incubated for 1 h with 1 ml of nickel-nitrilotriacetic acid Superflow beads (QIAGEN, Valencia, CA) per 50 ml of lysate. The nickel-nitrilotriacetic acid medium was packed into an FPLC column, and the RNase H1 proteins were partially purified with sequential gradients (flow rate, 5 ml/min; buffer A, 100 mM sodium phosphate, 10 mM Tris-HCl, and 8 M urea, pH 6.3; buffer B, 100 mM sodium phosphate, 10 mM Tris-HCl, and 2 M urea, pH 6.3; buffer C, 100 mM sodium phosphate, 10 mM Tris-HCl, 2 M urea, and 100 mM EDTA, pH 7.0). The eluent was further purified by ion exchange FPLC chromatography using a Mono S column (GE Healthcare, Uppsala, Sweden); flow rate, 1 ml/min; buffer A, 20 mM sodium phosphate, 2 M urea, and 200 mM NaCl, pH 7.0; buffer B, 20 mM sodium phosphate, 2 M urea, and 2 M NaCl, pH 7.0. Fractions containing RNase H1 were pooled and concentrated. The concentrated protein was purified by reversed-phase, fast-performance liquid chromatography using Resourse RPC Column (GE Healthcare); flow rate, 1 ml/min; buffer A, 2% acetonitrile in deionized water and 0.065% trifluoroacetic acid; buffer B, 80% acetonitrile in deionized water and 0.05% trifluoroacetic acid. Fractions were lyophilized, resuspended in deionized water and analyzed by SDS-polyacrylamide gel electrophoresis.

Synthesis of Oligonucleotides. Synthesis and purification of chimeric 2′-methoxyethoxy/deoxy oligoribonuceotides were as described previously (Baker et al., 1997; Mckay et al., 1999). The oligoribonucleotides were synthesized on a PE-ABI 380B synthesizer using 5′-*O*-silyl-2′-*O*-bis(2-acetoxyethoxy)methyl ribonucleoside phosphoramidites and procedures described elsewhere (Scaringe, 1998). The oligoribonucleotides were purified by reversed-phase HPLC. The oligodeoxyribonucleotides were synthesized on a PE-ABI 380B automated DNA synthesizer and standard phosphoramidite chemistry. The oligodeoxyribonucleotides were purified by precipitation twice in 0.5 M NaCl with 2.5 volumes of ethyl alcohol. The purified products were greater than 90% full-length material as determined by polyacrylamide gel electrophoresis analysis.

Preparation of ^{32}P labeled substrate. The RNA substrate was 5′-end-labeled with ^{32}P using 20 U of T4 polynucleotide kinase (Promega, Madison, WI), 120 pmol (7000 Ci/mmol) of [γ-^{32}P]ATP (MP Biomedicals, Irvine, CA), 40 pmol of RNA, 70 mM Tris, pH 7.6, 10 mM $MgCl_2$, and 50 mM DTT. The kinase reaction was incubated at 37°C for 30 min. The labeled oligoribonucleotide was purified by electrophoresis on a 12% denaturing polyacrylamide gel (Sambrook et al., 1989). The specific activity of the labeled oligonucleotide was approximately 3000 to 8000 cpm/fmol.

Preparation of the Heteroduplexes. The heteroduplex substrate was prepared in 100 μl containing 500 nM unlabeled oligoribonucleotide, 10^5 cpm of ^{32}P-labeled oligoribonucleotide, a 2-fold excess of complementary oligodeoxyribonucleotide and hybridization buffer (20 mM Tris, pH 7.5, and 20 mM KCl). Reactions were heated at 90°C for 5 min, cooled to 37°C. Hybridization reactions were incubated 2 - 16 h at 37°C and 1 mM tris(2-carboxyethyl)phosphine hydrochloride, 1 mM $MgCl_2$ and 60 U of Prime RNase Inhibitor (Eppendorf North America, Westbury, NY) was added.

Multiple-Turnover Kinetics. The human RNase H1 proteins were incubated with dilution buffer (50 mM tris, 50 mM NaCl, and 100 μM tris(2-carboxyethyl)phosphate, pH 7.5) for 1 h at 37°C. The heteroduplex substrate was digested with 0.4 ng of enzyme at 37°C. A 10-μl aliquot of the cleavage reaction was removed at time points ranging from 2 to 120 min and quenched by adding 10 μl of stop solution (8 M urea and 120 mM EDTA). The aliquots were heated at 90°C for 2 min, resolved in a 12% denaturing polyacrylamide gel, and the substrate and product bands were quantitated on a PhosphorImager (GE Healthcare). The concentration of the converted product was plotted as a function of time. The initial cleavage rate (V_0) was obtained from the slope (nmol RNA cleaved/min) of the best-fit line for the linear portion of the plot, which comprises, in general $<$10% of the total reaction and data from at least five time points.

Cell Culture and Treatment. ASOs were transfected into mouse brain endothelial (bEND) cells, obtained from the American Type Culture Collection (Manassas, VA), using 3 μg/ml lipofectin (Invitrogen, Carlsbad, CA) in OptiMem (Invitrogen) for 4 h. Transfection mixes were then exchanged with normal growth medium (high-glucose Dulbecco's modified Eagle's medium containing 10% fetal bovine serum, all from Invitrogen) and cells incubated for 48 h before RNA harvest. RNA was purified using an RNeasy 96-well plate

(QIAGEN) according to manufacturer's protocol and eluted in water. RNA was analyzed by quantitative reverse transcription-PCR using an ABI Prism 7700 (Applied Biosystems, Foster City, CA). TRADD RNA levels were normalized to those of cyclophilin A, a housekeeping gene. Primers used for determination of TRADD RNA level are as follows: forward, 5′-GGCCGCCTGCCAGAC-3′; reverse, 5′-TGAAGAGTCAGTGGCCGGTT-3′; probe, 5′–6-carboxyfluorescein-TTTCTGTTCCACGGGCAGCTCGTAGT–5-carboxytetramethylrhodamine-3′. Primers used for determination of cyclophilin A RNA level are as follows: forward, 5′-TCGCCGCTTGCTGCA-3′; reverse, 5′-ATCGGCCGTGATGTCGA-3′; PR, 5′-carboxyfluorescein–CCATGGTCAACCCCACCGTGTTC-5-carboxytetramethylrhodamine-3′. Values shown represent the average ± S.D. (n = 3 per treatment group).

Results

Effects of Successive MOE Substitutions Positioned at the 3′ and 5′ Poles of the ASO. The cleavage sites of the heteroduplex A substrates in which the deoxyribonucleotides were successively substituted with MOE-modified residues at the 3′ pole of the ASO are shown in Fig. 1A. Human RNase H1 cleavage of the unmodified heteroduplex A resulted in a broad cleavage pattern consisting of 10 cleavage sites with the 5′-most and 3′-most cleavage sites 6 and 15 residues, respectively, from the 5′ terminus of the oligoribonucleotide (Fig. 1A). The unmodified heteroduplex A also exhibited several preferred human RNase H1 cleavage sites; i.e., sites cleaved 2- to 3-fold faster than other sites by the enzyme. For example, preferred cleavage sites were observed at ribonucleotides 7, 8, 9, 11, and 15 from the 5′ terminus of the RNA. Heteroduplexes in which the first one or two 3′-nucleotides were MOE residues (19-1 and 18-2) exhibited a similar number of cleavage sites compared with the unmodified heteroduplex (Fig. 1A). Ablation of the 5′-most cleavage site in the oligoribonucleotide was observed for the heteroduplex containing three MOE residues at the 3′ terminus of the ASO (Fig. 1A). Each additional MOE substitution resulted in a concomitant ablation of the 5′-most cleavage site in the oligoribonucleotide, resulting in a separation of four to five base

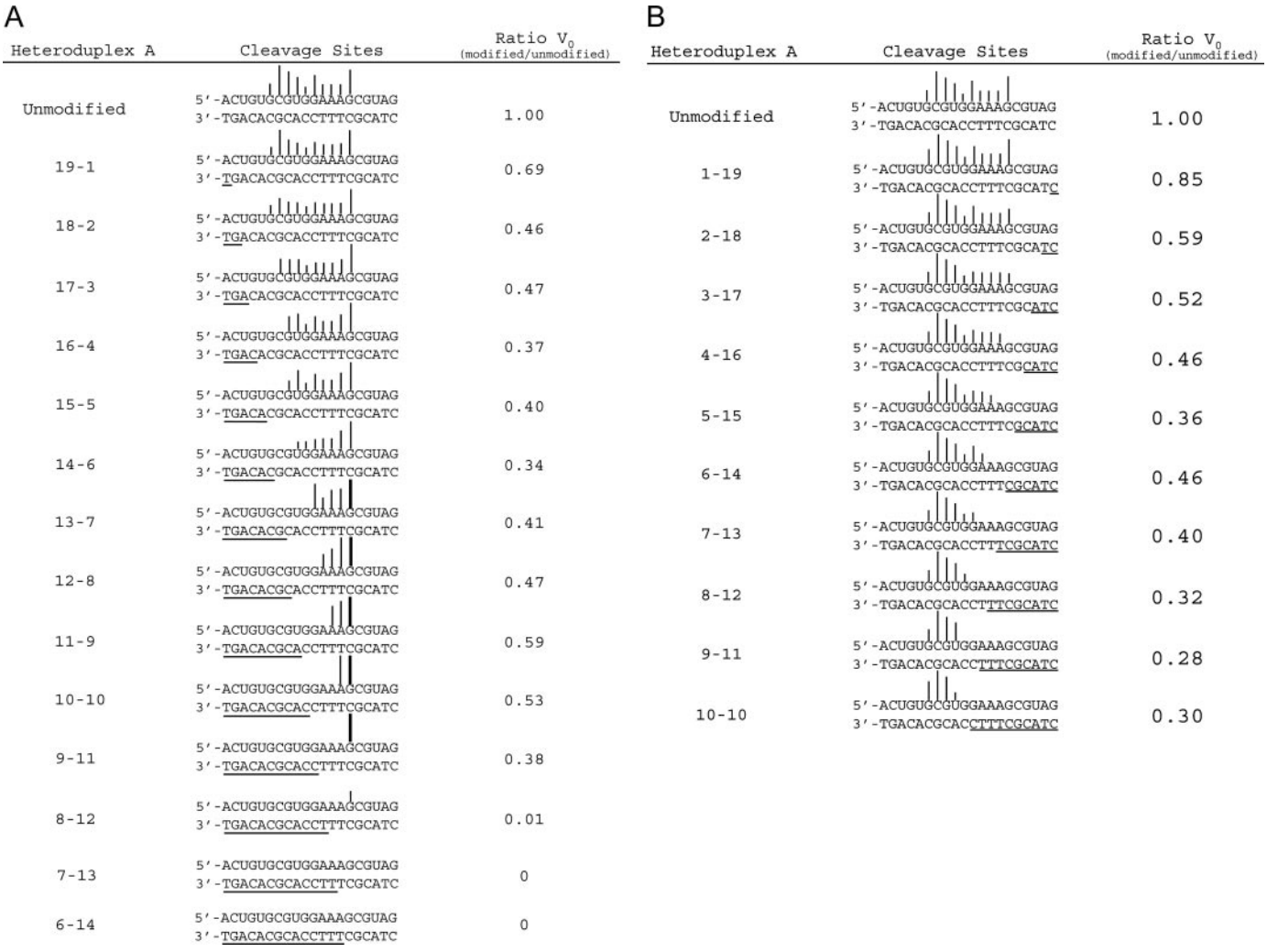

Fig. 1. Relative human RNase H1 initial cleavage rates and cleavage sites for the modified heteroduplex substrates. A, successive substitution of MOE-modified nucleotides at the 3′ pole of the ASO. B, successive substitution of MOE-modified nucleotides at the 5′ pole of the ASO. Lines indicate the position of the human RNase H1 cleavages on the heteroduplex substrate. The length and thickness of the lines represent the intensity of the bands on the denaturing polyacrylamide gel for each respective cleavage site. Longer and thicker lines correspond to bands exhibiting greater intensity. Underlined sequences indicate the position of the MOE modified nucleotides. Heteroduplexes are shown with the sense oligoribonucleotide (above) oriented 5′→3′ and chimeric ASO (below) 3′→5′. Ratio V_0 represents the initial cleavage rates for the modified heteroduplexes divided by the unmodified substrate. The V_0 values are an average of three measurements with estimated errors of CV <10%. Initial cleavage rates were determined as described under *Materials and Methods*.

pairs between the 5′-most cleavage site and the 5′-terminal MOE residue with greater than 11 MOE substitutions, resulting in the loss of all the human RNase H1 cleavage sites.

The cleavage rate for the 19-1 heteroduplex containing a single MOE positioned at the 3′ terminus of the ASO was 31% slower than the unmodified heteroduplex A (Fig. 1A). Two MOE substitutions at the 3′ terminus of the ASO (18-2) resulted in a cleavage rate approximately 50% slower than the cleavage rate for the unmodified heteroduplex. No further reduction in the cleavage rate was observed for the heteroduplexes containing 3 to 11 MOE residues at the 3′ pole of the ASO irrespective of the number of cleavage sites. In addition, the MOE residues at the 3′ pole of the ASO produced new preferred cleavage sites 3′ on the RNA (Fig. 1A). For example, one human RNase H1 cleavage site on the 11–9 heteroduplex accounted for an initial cleavage rate comparable with the 16-4 heteroduplex with eight cleavage sites.

The effect of MOE substitutions at the 5′ pole of the ASO on the cleavage patterns and initial cleavage rates are shown in Fig. 1B. Similar numbers of cleavage sites were observed for the unmodified substrate and heteroduplexes containing one to three MOE residues at the 5′ terminus of the ASO (Fig. 1B). Four MOE residues at the 5′ pole of the ASO resulted in the ablation of the 3′-cleavage site on the RNA. Additional MOE substitutions at the 5′ pole of the ASO resulted in a concomitant ablation of the 3′-most cleavage site in the RNA (Fig. 1B). The cleavage pattern for the heteroduplexes containing greater than three MOE residues at the 5′ pole of the oligodeoxyribonucleotide showed a consistent separation of two base pairs between the 3′-cleavage site on the RNA and the 3′-terminal MOE nucleotide on the ASO (Fig. 1B). In contrast to the observations with MOE modifications positioned at the 3′ pole of the oligodeoxyribonucleotide, fewer cleavage sites resulted in slower overall cleavage rates. For example, a 70% reduction in the cleavage rate was observed for the 10-10 heteroduplex containing three cleavage sites compared with the unmodified substrate with 10 cleavage sites. In this case, the successive ablation of the 5′-most cleavage sites did not produce an enhanced rate for the remaining cleavage sites. Finally, similar reductions in the cleavage rates were observed for the heteroduplexes containing two MOE substitutions at either the 3′ or 5′-termini of the ASO (Fig. 1, A and B).

Effects of Heteroduplex Length. Given that the MOE substitutions at the 3′ and 5′ poles of the ASO effectively shortened the length of the RNA/DNA region of the chimeric substrates, we evaluated the influence of RNA/DNA length on human RNase H1 activity (Fig. 2). In particular, the sequence of the heteroduplex A was either shortened (A-10 and A-15) or extended (A-30 and A-40) from the 3′-RNA/5′-DNA terminus of the parent 20-base-pair sequence (A-20) (Fig. 2). The 5′-most cleavage site was consistently positioned six ribonucleotides from the 5′ terminus of the RNA. In contrast, the position of the 3′-most cleavage site on the RNA was dependent on the length of the heteroduplex. For example, the 3′-cleavage sites for the 10- and 15-base-pair heteroduplexes were positioned four ribonucleotides from the 3′ terminus of the RNA, whereas the distance between the 3′-most cleavage site and the 3′ terminus of the RNA increased to 6, 7, and 10 ribonucleotides for the 20-, 30-, and 40-base-pair substrates, respectively (Fig. 2). The positions of the preferred cleavage sites were also dependent on the length of the heteroduplex. The greatest human RNase H1 activity was observed at ribonucleotides 6 and 7 from the 5′ terminus of the RNA for the 10 base pair heteroduplex and ribonucleotides 6, 7, 8, and 11 for the 15-base-pair substrate. Additional preferred cleavage sites were observed 3′ on the RNA for the 20-, 30-, and 40-base-pair substrates. For example, preferred cleavage sites were observed at ribonucleotides 21 and 23 for the 30-base-pair heteroduplex and 30, 33, and 34 for the 40-base-pair heteroduplex.

Effects of Heteroduplex Sequence. The cleavage patterns and cleavage rates for various RNA/DNA heteroduplex sequences are shown in Fig. 3A. Heteroduplex A exhibited an unusually broad cleavage pattern with numerous preferred cleavage sites (Fig. 1). This unique cleavage pattern resulted in the greatest initial cleavage rate among the heteroduplexes tested. In contrast, the other heteroduplexes displayed a narrower cleavage pattern with fewer preferred cleavage sites positioned predominantly within the preferred position for cleavage (i.e., 7 to 12 ribonucleotides from the 5′ terminus of the RNA). Slower cleavage rates (~2-fold)were observed for these heteroduplexes compared with the heteroduplex A substrate.

Effects of 2′-MOE Substitutions Positioned at Both the 3′ and 5′ Poles of the ASO. Cleavage sites and rates for the chimeric heteroduplexes in which the RNA/DNA region was positioned either centrally (5-10-5) or toward the 3′ pole of the RNA (25-10-8) are shown in Fig. 3A. The cleavage sites for the 5-10-5 heteroduplexes were shifted 3′ on the RNA compared with the unmodified substrates. A further shift 3′ in the RNA was observed for the cleavage sites of the 25-10-8 heteroduplexes (Fig. 3A). Consistent with the successive

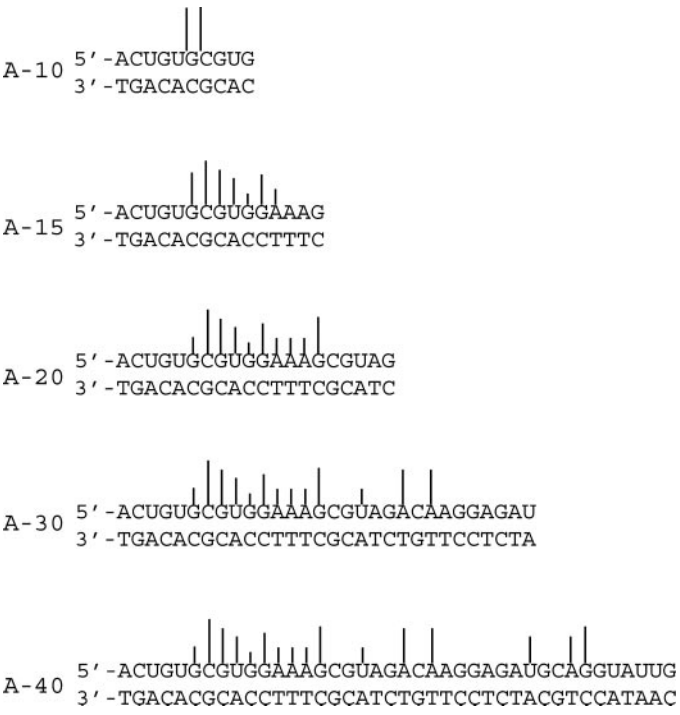

Fig. 2. Cleavage pattern for heteroduplex A of various lengths. Lines indicate the position of the human RNase H1 cleavages on the heteroduplex substrate. The length of the lines represents the intensity of the bands on the denaturing polyacrylamide gel for each respective cleavage site. Longer lines correspond to bands exhibiting greater intensity. Heteroduplexes are shown with the sense oligoribonucleotide (above) oriented 5′→3′ and the oligodeoxyribonucleotide (below) 3′→5′.

MOE substitutions in the ASO (Fig. 1A), the 5-10-5 and 25-10-8 heteroduplexes exhibited a separation of four to five base pairs from the 5′-most cleavage site on the RNA and the nearest MOE at the 3′ pole of the ASO (Fig. 3A). Likewise, a separation of two base pairs was observed between the 3′-most cleavage site on the RNA and the nearest MOE at the 5′ pole of the ASO. The greatest loss in human RNase H1 activity compared with the unmodified substrate was observed for the 5-10-5 chimeric heteroduplex A. The reduction in activity seemed to be due to the failure to generate a preferred cleavage site within the RNA/DNA portion of the chimeric substrate. Likewise, no preferred cleavage sites were observed for either the 5-10-5 or 25-10-8 heteroduplexes D, resulting in a reduction of >2-fold in the initial cleavage rate compared with the unmodified heteroduplex D, even though both chimeric heteroduplexes exhibited a greater number of cleavage sites compared with the unmodified heteroduplex D (Fig. 3A). In the case of heteroduplex C, new preferred cleavage sites were observed for the 5-10-5 heteroduplex, resulting in a cleavage rate comparable with the unmodified heteroduplex, whereas the 25-10-8 heteroduplex showed fewer cleavage sites, resulting in a 3-fold slower cleavage rate compared with either the 5-10-5 or unmodified heteroduplexes. In contrast, the 5-10-5 chimeric heteroduplex B exhibited a similar number of preferred cleavage sites compared with the unmodified heteroduplex B, resulting in an initial cleavage rate comparable with the unmodified substrate. Again, the number of preferred cleavage sites seems to have a greater effect on the initial cleavage rates for the various chimeric heteroduplexes than the total number of cleavage sites.

The sequences were chosen based on active ASO binding sites identified from ASO transfection of cultured cells (data not shown). To compare the effects of MOE substitutions in the ASO on human RNase H1 activity with the gene-silencing activities of the ASOs in cells, we transfected the 5-10-5 and 25-10-8 ASOs of heteroduplex C into bEND cells and measured the intracellular concentrations of the target mRNA, in this case TRADD mRNA. The heteroduplex C ASOs were chosen because these heteroduplexes showed the greatest difference in human RNase H1 activity for ASOs containing the same number of MOE residues and therefore

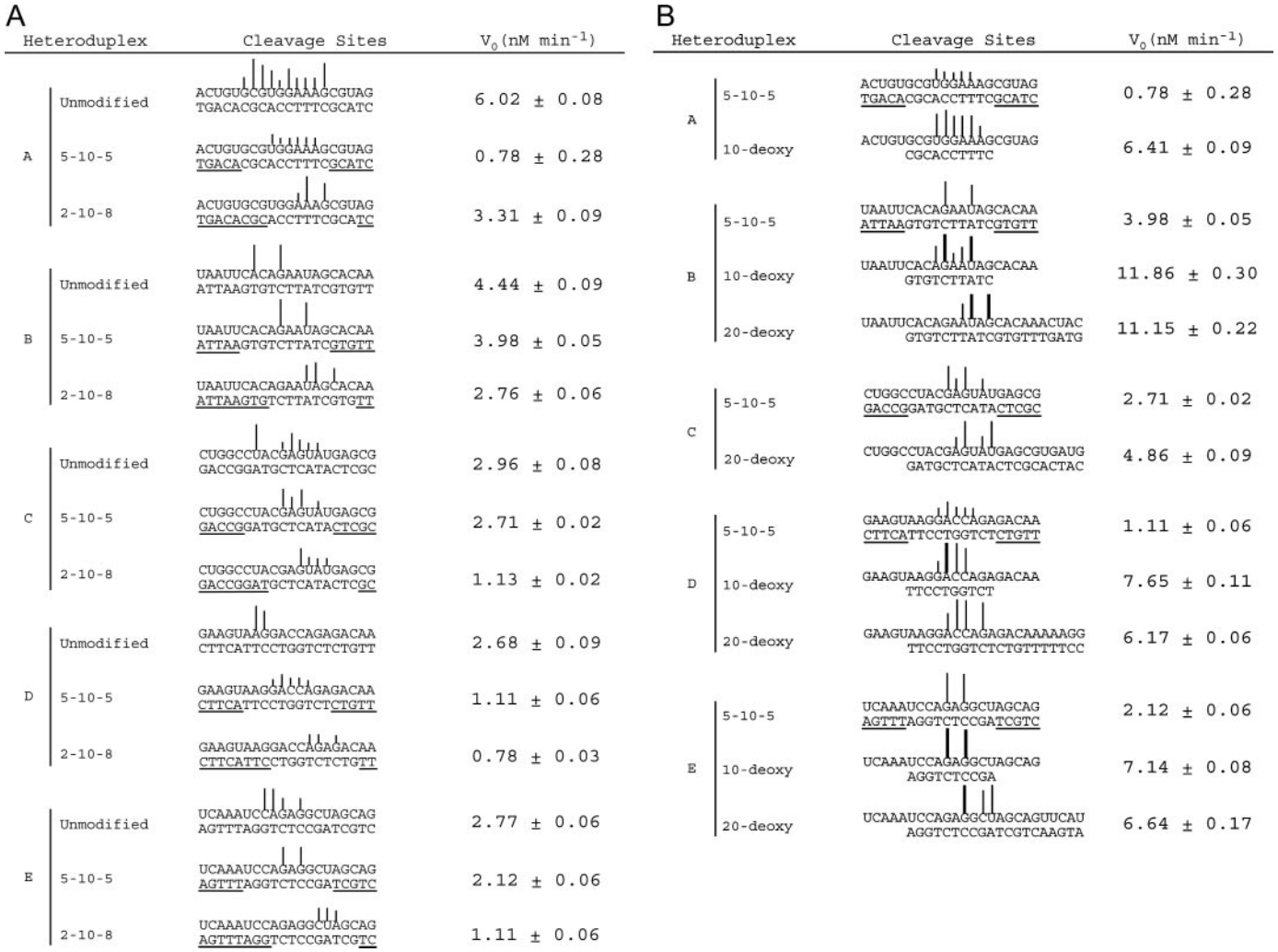

Fig. 3. Initial cleavage rates and cleavage sites for chimeric ASO configurations of various heteroduplex sequences. A, initial cleavage rates (V_0) and cleavage sites for heteroduplexes containing unmodified, 5-10-5 and 25-10-8 chimeric ASOs. B, initial cleavage rates and cleavage sites for heteroduplexes containing chimeric and unmodified ASO with similar 3′-DNA termini. Lines and underlined sequences are as described in Fig. 1. Heteroduplexes are shown with the sense oligoribonucleotide (above) oriented 5′→3′ and chimeric ASO (below) 3′→5′. The initial cleavage rates were determined as described in Fig. 1.

probably exhibit similar binding affinities for the mRNA target (Fig. 3A). Consistent with the reduction in cleavage rate observed for the 25-10-8 heteroduplex C compared with either the 5-10-5 or unmodified heteroduplexes, the 25-10-8 ASO was also less potent than the 5-10-5 ASO at reducing TRADD mRNA levels in the cell (Fig. 4). It is noteworthy that a greater reduction in activity was observed in cells; e.g., a 6-fold difference in IC_{50} was observed for the 25-10-8 and 5-10-5 ASOs compared with the 3-fold difference in the human RNase H1 cleavage rate (Figs. 3A and 4).

To evaluate both the influence of the MOE modifications and the contribution of heteroduplex sequence on human RNase H1 cleavage rates, unmodified heteroduplexes were prepared with the 5′ termini of the ASO positioned to match the 3′-MOE/5′-DNA junction of the 5-10-5 chimeric heteroduplexes (Fig. 2B). The length of the ASO was either 10 nucleotides to match the DNA portion of the 5-10-5 chimeric oligodeoxyribonucleotide or 20 nucleotides to match the unmodified substrate. In all cases, the initial cleavage rates for the unmodified heteroduplexes were significantly greater than the cleavage rates observed for the 5-10-5 heteroduplexes (Fig. 3B). Although similar cleavage patterns were observed for the 5-10-5 heteroduplexes and the unmodified heteroduplexes containing 10 deoxyribonucleotides, the RNase H1 activity at the cleavage sites of the unmodified heteroduplexes containing 10 deoxyribonucleotides was significantly greater compared with the 5-10-5 heteroduplexes. For example, two cleavage sites were observed for the 5-10-5 and unmodified heteroduplexes B and E containing 10 deoxyribonucleotides. However, the unmodified substrates exhibited significantly greater human RNase H1 activity at those sites, resulting in a 3-fold increase in the initial cleavage rates compared with the 5-10-5 chimeric heteroduplexes. In contrast, the heteroduplexes containing 20 deoxyribonucleotides exhibited additional cleavage sites 3′ on the RNA compared with the 5-10-5 and 10-deoxyribonucleotide heteroduplexes, although comparable cleavage rates were observed for the unmodified heteroduplexes containing 10 and 20 deoxyribonucleotides (Fig. 3B). These data suggest that the slower cleavage rates observed for the 5-10-5 heteroduplexes compared with the unmodified substrates were due to the MOE substitutions and not to the length of the deoxyribonucleotide region of the ASO.

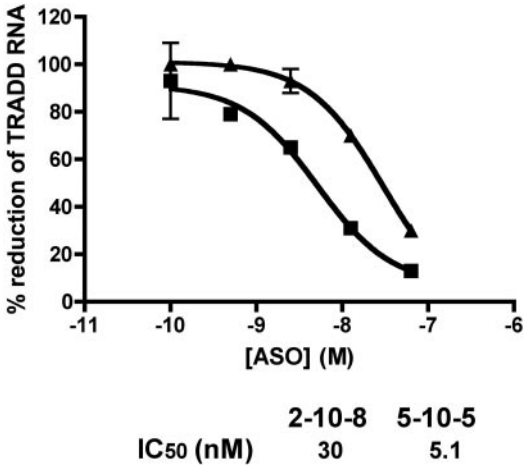

Fig. 4. Potency of heteroduplex C 5-10-5 and 25-10-8 ASOs in cultured cells. bEND cells were transfected with the 5-10-5 and 25-10-8 anti-TRADD ASOs of heteruplex C as described under *Materials and Methods*. The TRADD mRNA levels were determined for various ASO concentrations by quantitative RT-PCR. Results were plotted with percent normalized mRNA versus ASO concentrations for the 5-10-5 ASO (■) and the 25-10-8 ASO (▲). The bars represent S.D. of the mean of three treatment groups. IC_{50} (shown bellow the graph) were calculated from nonlinear least-squares fit of the data.

Okazaki-like substrates were prepared with a oligodeoxyribonucleotide annealed to a complementary RNA/DNA chimeric oligonucleotide containing 10 (A-10/10) and 15 (A-15/5) ribonucleotides at the 5′ pole and 10 and 5 contiguous deoxyribonucleotides, respectively, extending 3′ (Fig. 5). Deoxyribonucleotide substitutions at the 3′ pole of the oligoribonucleotide resulted in a loss of the 3′-most cleavage site and an increase in the cleavage rates for the remaining sites (Fig. 5). In other words, the successive ablation of the 3′-most cleavage sites produced new preferred cleavage sites, resulting in comparable cleavage rates for the A-10/10, A-15/5, and unmodified heteroduplexes.

Discussion

Heteroduplex Sequence and Structure Affect Cleavage Sites and Rates. Certain human RNase H1 cleavage sites seemed to be preferentially cleaved, exhibiting 2- to 3-fold greater activity compared with the other cleavage sites (Figs. 1–3). In addition, these preferred cleavage sites provided the greatest contribution to the overall cleavage rate. No consensus sequence was observed for the preferred human RNase H1 cleavage sites (Figs. 1–3). Instead, the position of the preferred cleavage sites in the heteroduplex substrate is consistent with the strong positional preference for cleavage observed for the enzyme; i.e., human RNase H1 preferentially cleaves the heteroduplex substrate 7 to 10 nucleotides from the 5′-RNA/3′-DNA terminus (Wu et al., 1999; Lima et al., 2003a). Except for heteroduplex A, the preferred cleavage sites observed for the various heteroduplex sequences were positioned within this 7- to 10-nucleotide region (Fig. 3A).

The lack of a consensus sequence for the preferred cleavage sites is probably due to the binding interaction between the enzyme and substrate that is predicted to comprise approximately one helical turn of the heteroduplex substrate (Lima et al., 2003b, 2004). Consequently, the preferred cleavage sites are the product of the sequence/helical geometry of the heteroduplex region interacting with the enzyme. Consistent with these observations, proteins involved in the small-interfering RNA pathway have been shown to measure subtle sequence-dependent differences in the helical geometry of oligoribonucleotide duplexes (Tomari et al., 2004). For example, the Dicer-2/R2D2 heterodimer was shown to orient the small-interfering RNA for loading into the RNA-induced silencing complex based on subtle thermodynamic differences of the terminal base pairs. The complexity of these interactions is further emphasized by the results shown in Fig. 2. In theory, as the length of the heteroduplex was increased, cleavage sites should have expanded relatively uniformly, because all of the experiments were in substrate excess. In contrast, as the heteroduplexes were lengthened, we observed areas in which there was essentially no cleavage as well as new sites of preferred cleavages.

MOE Substitutions Inhibit Human RNase H1 Activity. The human RNase H1 cleavage rates for the chimeric

substrates containing deoxyribonucleotides flanked on both ends with MOE residues were slower than the cleavage rates observed for substrates containing similar RNA/DNA regions without MOE residues (Fig. 3). Several factors seem to contribute to the reduction in human RNase H1 activity. First, several chimeric heteroduplexes redirected the position of cleavage outside the positional preference for cleavage (e.g., the 25-10-8 chimeric heteroduplexes B, C, D, and E), resulting in fewer preferred cleavage sites and slower overall cleavage rates (Fig. 3A). It is noteworthy that the reduction in human RNase H1 activity observed for the 25-10-8 of heteroduplex C was consistent with a reduction potency observed for this ASO in cultured cells compared with the 5-10-5 ASO (Fig. 4).

Second, the reduction in human RNase H1 activity observed for the chimeric heteroduplexes seemed to be due primarily to the MOE substitutions and not to the shorter length of the deoxyribonucleotide region of the chimeric heteroduplexes, because comparable cleavage rates were observed for the heteroduplexes containing the 10 and 20 deoxyribonucleotides without flanking MOE residues (Fig. 3B). The influence of the MOE substitutions on human RNase H1 activity is consistent with the solution structure of a chimeric heteroduplex containing deoxyribonucleotides flanked on both ends with 2′-methoxy residues hybridized to RNA (Nishizaki et al., 1997). In particular, the central deoxyribonucleotides exhibited the eastern-biased sugar conformation preferred by RNase H1, whereas the flanking 2′-methoxy residues exhibited a northern sugar conformation. It is noteworthy that the deoxyribonucleotides adjacent to the 2′-methoxy residues also were shown to exhibit a northern sugar conformation, suggesting the conformational transmission of the northern-biased 2′-methoxy residues into adjacent deoxyribonucleotides (Nishizaki et al., 1997). Given that heteroduplexes containing northern-biased nucleotides within the DNA strand do not support human RNase H1 activity (Lima et al., 2004), the attenuation of the human RNase H1 activity observed for the chimeric heteroduplexes is probably due to the conformational transmission of the northern-biased MOE residues into the adjacent deoxyribonucleotides.

Third, the influence of the MOE residues on human RNase H1 activity was directional (Fig. 1). The observed differences in activity between chimeric heteroduplexes containing MOE residues at the 5′ pole of the DNA strand compared with the 3′ pole are probably due to the binding directionality of the enzyme. Human RNase H1 is predicted to position the catalytic domain 3′ on the RNA relative to the RNA binding-domain (Fig. 6). As a result, MOE substitutions at the 3′ pole of the oligodeoxyribonucleotide would be positioned at the RNA binding-domain, and the MOE modifications at the 5′ pole would be positioned adjacent to the catalytic domain of the enzyme (Fig. 6). Given that the RNA binding domain of human RNase H1 has been shown to be important for properly positioning the enzyme on the heteroduplex for catalysis (Lima et al., 2003a), MOE substitutions at the 3′ pole of the oligodeoxyribonucleotide probably interfere with the binding of the enzyme to this portion of the substrate, effectively redirecting the enzyme to the RNA/DNA region of the chimeric heteroduplex (Figs. 1A and 6). Consistent with this model, MOE substitutions at the 5′ pole of the oligodeoxyribonucleotide would interfere with the catalytic domain of the enzyme, resulting in the observed progressive ablation of human RNase H1 cleavage sites without the concomitant production of new preferred cleavage sites (Fig. 1B and 6).

Human RNase H1 Is Optimally Evolved to Cleave Okazaki Fragments. A recent study demonstrated that RNase H1 is required for mitochondrial DNA replication and plays a critical role in the embryonic development of mice (Ceritelli et al., 2003). The enzyme is believed to participate in the removal of RNA primers during lagging strand DNA synthesis (Busen et al., 1977; Turchi et al., 1994; Ceritelli et al., 2003). Therefore, the proposed native substrates for the enzyme are chimeric heteroduplexes consisting of 7 to 14 ribonucleotide primers with contiguous stretches of DNA extending 3′, hybridized to DNA (Bambara et al., 1997). Consistent with the proposed biological role for the enzyme, the Okazaki-like substrates containing 5 and 10 deoxyribonucleotides at the 3′ pole of the oligoribonucleotide produced new preferred cleavage sites and exhibited cleavage rates comparable with the unmodified heteroduplex (Fig. 5). Considering that the short RNA primers are interspersed within long stretches of dsDNA, the model proposed here for the interaction between the enzyme and the heteroduplex substrate correlates well with biological roles for the enzyme (Fig. 6). First, the strong positional preference for cleavage is consistent with the length of the RNA primers. Second, human RNase H1 binds the RNA/DNA heteroduplex ~50-fold tighter than dsDNA, suggesting that the enzyme would not be trapped in nonproductive interactions within the large field of dsDNA (Wu et al., 1999). Third, the limited sequence discrimination exhibited by the enzyme would be beneficial given that the RNA primers comprise mixed sequences. Fi-

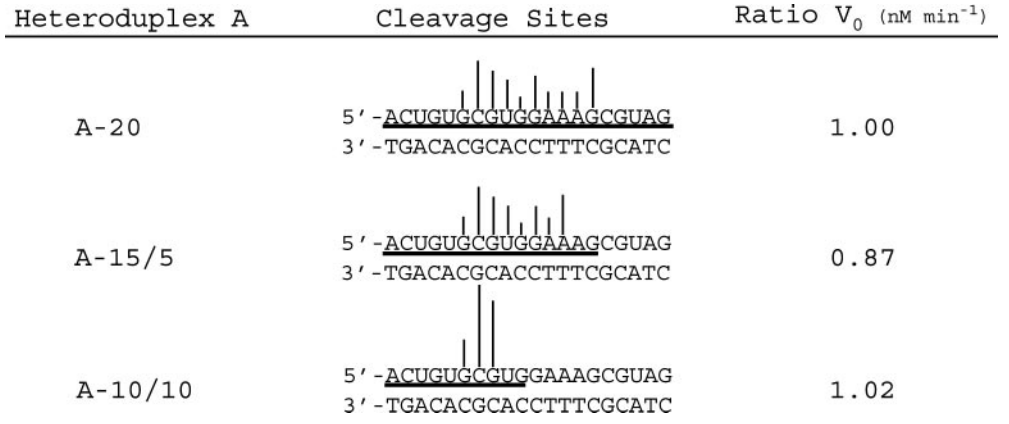

Fig. 5. Initial cleavage rates and cleavage sites for Okazaki-like substrates. Heteroduplexes are shown with the chimeric sense oligonucleotide (above) oriented 5′→3′ and oligodeoxyribonucleotide (below) 3′→5′. The underlined sequences indicate the positions of the ribonucleotide residues. The substrates consisted of heteroduplexes containing 10 (A-10/10) and 15 (A-15/5) ribonucleotides at the 5′ pole of the sense oligonucleotide with contiguous stretches of 10 and 5 deoxyribonucleotides, respectively, at the 3′ pole of the sense oligonucleotide. Lines are as described in Fig. 1. Ratio V_0 was determined as described in Fig. 1.

nally, DNA substitutions seemed to affect human RNase H1 activity differently than MOE substitutions. Although both the DNA and MOE substitutions resulted in a similar shift in the position of cleavage and few cleavage sites compared with the unmodified substrate, the MOE substitutions resulted in slower overall cleavage rates, whereas the DNA substitutions generated new preferred cleavage sites. The differences in activity are probably due to the differences in the sugar conformation as well conformational transmission of the MOE and DNA residues.

The Design of Improved DNA-Like ASOs. The observations presented here combined with the demonstration that human RNase H1 plays a dominant role in the activities of DNA-like ASOs offer approaches to enhance the design of effective chimeric ASOs (Lima et al., 2003b). Although the endogenous ASO/mRNA structures contain single-stranded RNA regions extending from both termini of the ASO, the cleavage patterns observed for the chimeric ASOs with flanking 2′-modifications suggest that these regions would have no effect on the activity of the enzyme (Fig. 3). In fact, cleavage sites identical to those observed for the 5-10-5 heteroduplex E were also observed for the endogenous target mRNA from human cells transfected with the 5-10-5 chimeric ASO of heteroduplex E using RNA ligase mediated rapid amplification of 5′-cDNA ends (Barnes, 1994) (data not shown). Most importantly, the observed influence of the MOE substitutions of on human RNase H1 activity suggests that reducing the number 2′- modified nucleotides should improve the enzyme activity. As 2′-modified nucleotides improve affinity to target RNA, reducing the number of 2′-modified nucleotides would obviously reduce the ability of the ASO to invade structured RNA sites, resulting in fewer active sites in the mRNA. However, once hybridization is accomplished, RNase H1 activity becomes limiting, so fewer 2′-MOE residues should result in greater ASO potency (Lima et al., 2003b). Finally, inserting modified nucleotides to modulate the transmission of the 2′-modified/RNA geometry into the RNA/DNA portion of the chimeric heteroduplex should also improve human RNase H1 activity.

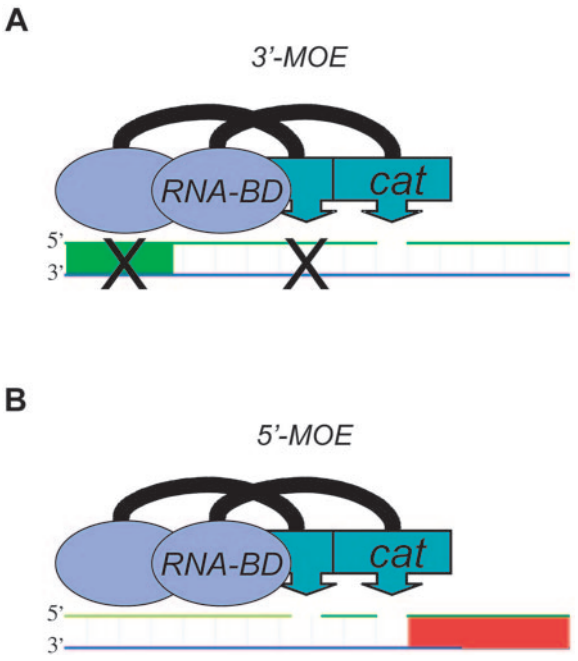

Fig. 6. Model for the interaction of RNase H1 with the heteroduplex substrate containing MOE modifications at the 3′ and 5′ poles of the ASO. The green and blue lines represent the sense oligoribonucleotide oriented 5′→3′ and chimeric ASO oriented 3′→5′, respectively. The green and red boxes represent MOE residues at the 3′ and 5′ poles, respectively, of the ASO. The binding interaction for human RNase H1 is shown with the RNA-binding domain (RNA-BD) of the enzyme positioned 5′ to the catalytic domain (Cat) on the oligoribonucleotide. Each observed cleavage site on the RNA is coupled to a specific binding interaction between the RNA-BD and the 3′-DNA/5′-RNA pole of the heteroduplex substrate. A, alteration in helical geometry or steric interference by the MOE substitutions at the 3′ pole of the ASO disrupts the binding interaction between the RNA-BD and the heteroduplex resulting in the observed ablation of catalytic activity at the 5′-most cleavage sites on the RNA. B, MOE substitutions at the 5′ pole of the ASO are positioned adjacent to the catalytic domain of enzyme.

References

Baker BF, Lot SS, Condon TP, Cheng-Flournoy S, Lesnik EA, Sasmor HM, and Bennett CF (1997) 2′-O-(2-Methoxy)ethyl-modified anti-intercellular adhesion molecule 1 (ICAM-1) oligonucleotides selectively increase the ICAM-1 mRNA level and inhibit formation of the ICAM-1 translation initiation complex in human umbilical vein endothelial cells. *J Biol Chem* **272:**11994–12000.

Bambara RA, Murante RS, and Hendriksen LA (1997) Enzymes and reactions at the eukaryotic DNA replication fork. *J Biol Chem* **272:**4647–4650.

Barnes WM (1994) PCR amplification of up to 35-kb DNA with high fidelity and high yield from lambda bacteriophage templates. *Proc Natl Acad Sci U S A* **91:**2216–2219.

Busen W, Peter JH, and Hausen P (1977) Ribonuclease H levels during the response of bovine lymphocytes to concanavalin A. *Eur J Biochem* **74:**203–208.

Busen W (1980) Purification, subunit structure, and serological analysis of calf thymus ribonuclease H I. *J Biol Chem* **255:**9434–9443.

Cerritelli SM and Crouch RJ (1995) The non-RNase H domain of Saccharomyces cerevisiae RNase H1 binds double-stranded RNA: magnesium modulates the switch between double-stranded RNA binding and RNase H activity. *RNA* **1:**246–259.

Ceritelli SM, Frolova EG, Feng C, Grinberg A, Love PE, and Crouch RJ (2003) Failure to produce mitochondrial DNA results in embryonic lethality in Rnaseh1 null mice. *Mol Cell* **11:**807–815.

Chi KN, Eisenhauer E, Fazli L, Jones EC, Powers J, Ayers D, Goldenberg SL, and Gleave ME (2004) A phase I pharmacokinetic (PK) and pharmacodynamic (PD) study of OGX-011, a 2′-methoxyethyl phosphorothioate antisense to clusterin, in patients with prostate cancer prior to radical prostatectomy [Abstract]. 2004 ASCO Annual Meeting Proceedings. *J Clin Oncol* **22 (Suppl 14S):**3033.

Crooke ST (2001) Basic principles of antisense technology, in *Antisense Drug Technology: Principles, Strategies, and Applications* (Crooke ST ed) pp 1–28, Marcel Dekker Inc, New York.

Crooke RM (2005) Antisense oligonucleotides as therapeutics for hyperlipidaemias. *Expert Opin Biol Ther* **7:**907–917.

Crouch RJ and Dirksen ML (1982) Ribonuclease H, in *Nucleases* (Linn SM and Roberts RJ eds) pp 211–241, Cold Spring Harbor Laboratory Press, Cold Spring Harbor, NY.

Eder PS, Walder RT, and Walder JA (1993) Substrate specificity of human RNase H1 and its role in excision repair of ribose residues misincorporated in DNA. *Biochimie* **75:**123–126.

Evans SP and Bycroft M (1999) NMR structure of the N-terminal domain of Saccharomyces cerevisiae RNase HI reveals a fold with a strong resemblance to the N-terminal domain of ribosomal protein L9. *J Mol Biol* **291:**661–669.

Frank P, Albert S, Cazenave C, and Toulme JJ (1994) Purification and characterization of human ribonuclease HII. *Nucleic Acids Res* **22:**5247–5254.

Itaya M and Kondo K (1991) Molecular cloning of a ribonuclease H (RNase HI) gene from an extreme thermophile Thermus thermophilus HB8: a thermostable RNase H can functionally replace the Escherichia coli enzyme in vivo. *Nucleic Acids Res* **19:**4443–4449.

Itaya M, McKelvin D, Chatterjie SK, and Crouch RJ (1991) Selective cloning of genes encoding RNase H from Salmonella typhimurium, Saccharomyces cerevisiae and *Escherichia coli* rnh mutant. *Mol Gen Genet* **227:**438–445.

Kanaya S, Katsuda-Kakai C, and Ikehara M (1991) Importance of the positive charge cluster in Escherichia coli ribonuclease HI for the effective binding of the substrate. *J Biol Chem* **266:**11621–11627.

Kanaya S and Itaya M (1992) Expression, purification, and characterization of a recombinant ribonuclease H from *Thermus thermophilus* HB8. *J Biol Chem* **267:**10184–10192.

Kastelein JJ, Wedel MK, Baker BF, Su J, Bradley JD, Yu RZ, Chuang E, Graham MJ, and Crooke RM (2006) Potent reduction of apolipoprotein B and low-density lipoprotein cholesterol by short-term administration of an antisense inhibitor of apolipoprotein B. *Circulation* **114:**1729–1735.

Katayanagi K, Miyagawa M, Matsushima M, Ishkiawa M, Kanaya S, Ikehara M, Matsuzaki T, and Morikawa K (1990) Three-dimensional structure of ribonuclease H from *E. coli*. *Nature (Lond)* **347:**306–309.

Kjems LL, Bhanot S, Bradley JD, Monia B, Kwoh J, and Wedel M (2005) Increased insulin sensitivity in humans by protein tyrosine phosphatase 1B (PTP-1B); inhibition-evaluation of ISIS 113715, an antisense inhibitor of PTP-1B. *Diabetes* **54 (Suppl. 1):**A530.

Lima WF, Nichols JG, Wu H, Prakash TP, Migawa MT, Wyrzykiewicz TK, Bhat B, and Crooke ST (2004) Structural requirements at the catalytic site of the heteroduplex substrate for human RNase H1 catalysis. *J Biol Chem* **279:**36317–36326.

Lima WF, Wu H, and Crooke ST (2001) Human RNases H. *Methods Enzymol* **341:**430–440.
Lima WF, Wu H, Nichols JG, Manalili SM, Drader JJ, Hofstadler SA, and Crooke ST (2003a) Human RNase H1 activity is regulated by a unique redox switch formed between adjacent cysteines. *J Biol Chem* **278:**14906–14912.
Lima WF, Wu H, Nichols JG, Prakash TP, Ravikumar V, and Crooke ST (2003b) Human RNase H1 uses one tryptophan and two lysines to position the enzyme at the 3′-DNA/5′-RNA terminus of the heteroduplex substrate. *J Biol Chem* **278:** 49860–49867.
Masutani C, Enomoto T, Suzuki M, Hanaoka F, and Ui M (1990) DNA primase stimulatory factor from mouse FM3A cells has an RNase H activity. Purification of the factor and analysis of the stimulation. *J Biol Chem* **265:**10210–10216.
Mckay R, Miraglia L, Cummins L, Owens S, Sasmor HM, and Dean NM (1999) Characterization of a potent and specific class of antisense oligonucleotide inhibitor of human protein kinase C-α expression. *J Biol Chem* **274:**1715–1722.
Nakamura H, ODA Y, Iwai S, Inoue H, Ohtsuka E, Kanaya S, Kimura S, Katsuda C, Katayanagi K, Morikawa K, et al. (1991) How does RNase H recognize a DNA.RNA hybrid? *Proc Natl Acad Sci U. S. A.* **88:**11535–11539.
Nishizaki T, Iwai S, Ohtsuka E, and Nakamura H (1997) Solution structure of an RNA. 2′-*O*-Methylated RNA hybrid duplex containing an RNA. DNA hybrid segment at the center. *Biochemistry* **36:**2577–2585.
Rong YW and Carl PL (1990) On the molecular weight and subunit composition of calf thymus ribonuclease H1. *Biochemistry* **29:**383–389.
Sambrook J, Fritsch EF, and Maniatis T (1989) *Molecular Cloning: A Laboratory Manual*, 2nd ed., Cold Spring Harbor Laboratory Press, Cold Spring Harbor, NY
Scaringe SA (2001) RNA oligonucleotide synthesis via 5′-silyl-2′-orthoester chemistry. *Methods* **23:**206–217.
Scaringe SA, Wincott FE, and Caruthers MH (1998) RNA oligonucleotide synthesis via 5′-silyl-2′-orthoester chemistry. *J Am Chem Soc* **120:**11820–11821
Stein H and Hausen P (1969) Enzyme from calf thymus degrading the RNA moiety of DNA-RNA Hybrids: effect on DNA-dependent RNA polymerase. *Science (Wash DC)* **166:**393–395.
Tomari Y, Matranga C, Haley B, Martinez N, and Zamore PD (2004) A protein sensor for siRNA asymmetry. *Science (Wash DC)* **306:**1377–1380.
Turchi JJ, Huang L, Murante RS, Kim Y, and Bambara RA (1994) Enzymatic completion of mammalian lagging-strand DNA replication. *Proc Natl Acad Sci U.S.A.* **91:**9803–9807.
Wu H, Lima WF, and Crooke ST (1998) Molecular Cloning and Expression of cDNA for Human RNase H. *Antisense Nucleic Acid Drug Dev* **8:**53–61.
Wu H, Lima WL, and Crooke ST (1999) Properties of cloned and expressed human RNase H1. *J Biol Chem* **274:**28270–28278.
Wu H, Lima WF, and Crooke ST (2001) Investigating the structure of human RNase H1 by site-directed mutagenesis. *J Biol Chem* **276:**23547–23553.
Wu H, Lima WF, Zhang H, Fan A, Sun H, and Crooke ST (2004) Determination of the role of the human RNase H1 in the pharmacology of DNA-like antisense drugs. *J Biol Chem* **279:**17181–17189.
Yacyshyn BR, Bowen-Yacyshyn MB, Jewell L, Tami JA, Bennett CF, Kisner DL, and Shanahan WR (1998) A placebo-controlled trial of ICAM-1 antisense oligonucleotide in the treatment of Crohn's disease. *Gastroenterology* **114:**1133–1142.
Yang W, Hendrickson WA, Crouch RJ, and Satow Y (1990) Structure of ribonuclease H phased at 2 A resolution by MAD analysis of the selenomethionyl protein. *Science (Wash DC)* **249:**1398–1405.

Address correspondence to: Walt F. Lima, 2292 Faraday Ave., Carlsbad, CA 92008. E-mail: wlima@isisph.com